J. Appl. Comput. Mech., 9(1) (2023) 195-204
DOI: 10.22055/jacm.2022.40757.3648

ISSN: 2383-4536
jacm.scu.ac.ir

Shahid Chamran University of Ahvaz

Journal of Applied and Computational Mechanics

Research Paper

Flow Structure when Filling a Channel with a Curable Liquid

Evgeny I. Borzenko[1], Gennady R. Shrager[2]

[1] Faculty of Physics and Engineering, Tomsk State University, 36, Lenin Ave., Tomsk, 634050, Russia, Email: borzenko@ftf.tsu.ru

[2] Faculty of Physics and Engineering, Tomsk State University, 36, Lenin Ave., Tomsk, 634050, Russia, Email: shg@ftf.tsu.ru

Received May 11 2022; Revised July 15 2022; Accepted for publication July 23 2022.
Corresponding author: E.I. Borzenko (borzenko@ftf.tsu.ru)

Abstract. The filling of a plane gap with a non-Newtonian fluid under non-isothermal conditions is considered by assuming viscous dissipation and curing reaction induced by the heat supplied through the walls of the gap. The rheology of the medium is described by the modified Cross-WLF model accounting for the effect of temperature, strain rate intensity, and the extent of a chemical reaction on the viscosity. The curing reaction kinetics is determined by the equation based on the n-th order reaction with self-acceleration. The problem is solved numerically using an original computational technique. The curable fluid flow structure is revealed to include three characteristic zones during the filling process: a fixed layer on the solid wall with a high degree of curing; a central “core” with an almost uniform distribution of characteristics; and a transition zone serving as a "lubricating" layer between two abovementioned zones. The structure is governed by heating of the fluid through the wall, since the heating affects the rheological characteristics of the medium and the rate of the cured layer formation. Analysis of the similarity criteria for the considered flow conditions shows that the fluid flows in a creeping regime ($Re < 0.01$); the temperature distribution is mainly affected by convective heat transfer ($Pe > 100$); the influence of dissipative heating and exothermic effect of the curing reaction is insignificant. The effect of curing on the mass distribution of the liquid portions entering through the inlet section is shown. The variation of the pressure distribution is analyzed at various flow conditions.

Keywords: non-Newtonian fluid, non-isothermal, curing, free surface, numerical simulation.

1. Introduction

Manufacturing of products from polymeric materials is characterized by complex hydrodynamic, thermophysical, and chemical processes. In the technology of their processing by the casting method, the filling of plane and axisymmetric molds is often involved. Specific features of the filling of molds by injection molding with account for complex rheology and non-isothermal conditions in the absence of phase and chemical transformations have been studied in detail and described in [1-6]. It is noted that the flow in the vicinity of the free surface front has fountain-like behavior, and far from the front, the flow is one-dimensional.

Polymeric materials capable of curing when heated are known as thermosetting plastics. Curing is a chemical process that induces irreversible transformations of liquid reactive oligomers or polymers into solid, infusible, and insoluble cross-linked polymers. Thermosets are widely used in aircraft- and shipbuilding, as well as in rocket science and in the production of construction materials. For these purposes, the technology of their processing requires considerable efforts due to numerous affecting factors [7]. For instance, high temperature of the processed medium ensures its low viscosity; on the other hand, high temperatures activate a chemical reaction that leads to the formation of crosslinks, increases viscosity, and provides poor processability.

Experimental studies show that the processing of curable materials is characterized by time-varying rheological parameters and is accompanied by a change in its phase state, for example, gelation or glass transition [8]. Moreover, the same material behaves differently under various processing conditions, which is clearly demonstrated by a TTT (time-temperature-transformation) diagram [9-10]. Mathematical formulation of the problems describing a process of the product molding from thermosets includes a system of differential equations of motion, continuity, energy, and chemical kinetics, which are completed by functional dependences of the material characteristics on processing conditions, as well as by initial and boundary conditions. Overview of the models of polymer curing and rheological models considering the effect of temperature, strain conditions, and the extent of a chemical reaction, is presented in [11-13]. The analytical solution to the problems on the flow of such media is impractical, and the physical modeling is a very time-consuming and complex process that does not allow one to obtain detailed information on characteristics of the material. Numerical simulation gives comprehensive information on the process studied; although, it also requires significant computational capabilities. Numerical simulation results for the filling of the cavities of various shapes with a curable material are described in [14-16]. Calculations are performed using the OpenFOAM and Moldex3D packages. The process of the mold filling with a curable resin is studied in [17]. Here, the curing stage follows the completed mold filling. The results of the modeling of curing resin flows, which occur in technologies for producing cases of microelectronic

Published online: August 04 2022

components, are presented in [18, 19]. The axisymmetric channel filling with a fluid, taking into account a chemical reaction, is considered in [20]. That being said, the level of development of mathematical models for curable liquid flows and the experience of their implementation are still insufficient.

This work aims to numerically study the process of the plane channel filling with a non-Newtonian fluid considering the curing reaction induced by the heat supplied through a solid wall. It would appear that our study is the first to distinguish the flow structures of a curable liquid during the plane channel filling.

2. Formulation of the Problem

A plane gap flow with a free surface of a non-Newtonian fluid curing due to a heat-supply through the wall is considered. The flow region and the coordinate system are schematically shown in Fig. 1. In the considered temperature ranges and degrees of transformation, the density and the thermal conductivity are assumed to vary insignificantly and are specified by constant values, while the heat capacity depends on temperature. A mathematical formulation of the problem is written with account for dissipative heating and thermal effects of the curing reaction. Due to the symmetry of the problem, half of the flow region is considered. The fluid flows against gravity.

The flow is described by a system of momentum, continuity, and energy equations

$$\begin{gathered}\rho\left(\frac{\partial \mathbf{U}}{\partial t}+(\mathbf{U}\cdot\nabla)\mathbf{U}\right)=-\nabla P+\nabla\cdot\left(\eta\left(\nabla\mathbf{U}+\nabla\mathbf{U}^{T}\right)\right)+\rho\mathbf{g},\\ \nabla\cdot\mathbf{U}=0,\\ c\rho\left(\frac{\partial T}{\partial t}+(\mathbf{U}\cdot\nabla)T\right)=\lambda\nabla^{2}T+\Phi+\rho\Delta H\frac{\partial\alpha}{\partial t},\end{gathered} \tag{1}$$

where $\mathbf{g}=(0,-g)$. The degree of cure is determined by the Kamal kinetic equation [21], which is based on the n-th order reaction with self-acceleration

$$\begin{gathered}\frac{\partial\alpha}{\partial t}+(\mathbf{U}\cdot\nabla)\alpha=\left(k_1+k_2\alpha^{m}\right)(1-\alpha)^{n},\\ k_1=A\exp\left(-\frac{E_a}{RT}\right),\ k_2=B\exp\left(-\frac{E_b}{RT}\right).\end{gathered} \tag{2}$$

The mathematical formulation of the problem is completed by a rheological equation, according to which the apparent viscosity is determined by the following expression:

$$\begin{gathered}\eta(\dot\gamma,T,\alpha)=\frac{\eta_0(T)}{1+\left(\dfrac{\eta_0(T)\dot\gamma}{\sigma}\right)^{1-k}}\left(\frac{\alpha_g}{\alpha_g-\alpha}\right)^{C_1+C_2\alpha},\\ \eta_0(T)=C\exp\left(\frac{T_b}{T}\right).\end{gathered} \tag{3}$$

The first factor describes dependence of the viscosity on strain conditions and temperature in compliance with the Cross-WLF rheological model [22, 23], and the second factor, dependence on the degree of cure in compliance with the Castro Macosko model [24]. The selected rheological model is often used to describe the behavior of curable polymers in various engineering applications.

The mathematical formulation includes the boundary and initial conditions. In the inlet section Γ_2, the fluid is supplied at a given flow rate and zero degree of cure. The velocity and temperature profiles correspond to a steady-state one-dimensional fluid flow with aforementioned rheology at a wall temperature equaled to T_e and are determined by a one-dimensional problem solution. On the solid wall Γ_3, the no-slip condition is used, and the fluid temperature is determined by formula

$$T=\begin{cases}T_e+\dfrac{T_w-T_e}{3L}y,\ 0\le y\le 3L,\\ T_w,\ y>3L.\end{cases} \tag{4}$$

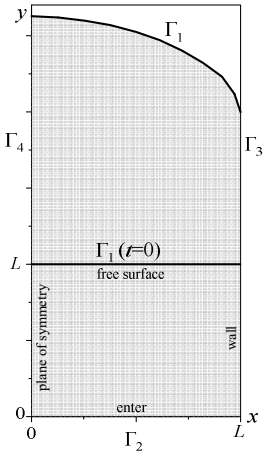

Fig. 1. Flow region and coordinate system

The value of T_w ensures the proceeding of the chemical reaction. In the inlet vicinity, a linear temperature increase from T_e to T_w in a pipe section of length 3L prevents the flow from the cured layer formation on the wall in this region. On the free surface Γ_1, the condition of the absence of shear stress is assigned, and the normal stress is set equal to the external pressure, which is equaled to zero without loss of generality; a zero heat flux is specified on the surface. Capillary effects are not considered. The motion of the boundary is described by a kinematic condition. At the initial time instant, the channel is partially filled with the fluid up to a height L; the surface has a plane horizontal shape; the temperature of the medium in the flow region is equal to T_e; the degree of cure is set to zero. On the symmetry plane Γ_4, symmetry conditions are specified.

The governing equations are rewritten in dimensionless variables. The following scales are used to make dimensionless the length, velocity, time, viscosity, pressure, and heat capacity: a half-width of the gap L, the average flow velocity in the inlet section U_0, L/U_0, $\eta_s = \eta(U_0/L, T_0, 0)$, $\eta_s U_0/L$, and c_0, respectively. The dimensionless temperature is introduced as follows: $\theta = (T - T_0)/T_0$; where T_0 is the temperature scale. Keeping the same notations for dissipation function and heat capacity, the system of equations (1) is rewritten as follows:

$$\begin{gathered} \mathrm{Re}\left(\frac{\partial \mathbf{u}}{\partial \tau} + (\mathbf{u}\cdot\nabla)\mathbf{u}\right) = -\nabla p + \nabla\cdot\left(\bar{\eta}\left(\nabla\mathbf{u} + \nabla\mathbf{u}^{\mathrm{T}}\right)\right) + \mathbf{W}, \\ \nabla\cdot\mathbf{u} = 0, \\ \mathrm{Pe}\left(c\frac{\partial\theta}{\partial\tau} + c(\mathbf{u}\cdot\nabla)\theta\right) = \nabla^2\theta + \mathrm{Br}\,\Phi + \mathrm{Da}\frac{\partial\alpha}{\partial \mathrm{t}}, \end{gathered} \tag{5}$$

where $\mathbf{W} = (0, -W)$. The problem formulation includes five dimensionless criteria

$$\mathrm{Re} = \frac{\rho U_0 L}{\eta_s},\ \mathrm{W} = \frac{\rho g L^2}{\eta_s U_0},\ \mathrm{Pe} = \frac{c_0 \rho U_0 L}{\lambda},\ \mathrm{Br} = \frac{\eta_s U_0^2}{\lambda T_0},\ \mathrm{Da} = \frac{\rho \Delta H U_0 L}{\lambda T_0}. \tag{6}$$

3. Solution Method

The flow region is discretized using a staggered grid, whose fragment is shown in Fig. 2. The problem is solved numerically with the use of the original approach based on the finite volume method and the SIMPLE algorithm [25] to satisfy the continuity equation. Difference analogs of the differential equations are written implicitly using the upwind scheme for convective terms, the central differences for diffusion terms, and Euler's scheme for time terms. The resulting system of algebraic equations is solved by the Gauss-Seidel method. The convergence of the iterative process in the SIMPLE procedure is estimated by the modulus of the pressure correction gradient. At irregular nodes near the free boundary (blue symbols in Fig. 2), the required variables are found by linear interpolation using the values from regular nodes (black symbols in Fig. 2) and free surface nodes (red symbols in Fig. 2).

The free surface is approximated by a set of markers which are arranged uniformly along the surface at the initial time instant. On the free surface, the dynamic boundary conditions are satisfied using the invariant method [26]. The movement of the markers is determined by difference analogs of the kinematic boundary condition. More details on the numerical algorithm are presented in [27].

As previously noted, when the gelation point is reached, the material loses its flow properties, and the apparent viscosity tends to infinity. In this regard, the rheological law is regularized in a similar way as in the case of viscoplastic fluids [28]. If the following condition is fulfilled in a finite volume

$$\alpha > \alpha_g - \varepsilon\ , \tag{7}$$

the volume is excluded from calculations of hydrodynamic flow characteristics. The regularization parameter ε is approved by a set of numerical experiments. The value must be small enough to provide the adequacy of the original model, and the iterative processes must converge in a reasonable time. As a result of test computations, the value ε = 0.025 is chosen for further calculations.

In parametric studies of the flow, the physical properties of the medium correspond to Vyncolit X655 glass fiber [16]: ρ = 2080 kg/m^3, α_g = 0,7 , $\sigma = 2.8\times10^{-9}$ Pa, k = 0.432, C_1 = 6.22, C_2 = -5.05, $C = 1.7\times10^5$ Pa.s, $T_b = 1.49\times10^4$ K, $A = 6.86\times10^6$ 1/s, $E_a = 9.29\times10^4$ J/mol, $B = 5.06\times10^6$ 1/s, $E_b = 8.52\times10^4$ J/mol, m = 0.892, n = 0.988, λ = 0.86 W/(m K), ΔH = 6529 J/kg and T_0 = 503 K. The heat capacity is determined by formula

$$c(T) = 2682.76 + 14.87\ T - 0.014\ T^2\ , \tag{8}$$

which represents an approximation of experimental data [16]. The heat capacity is scaled as follows: $c_0 = c(T_0)$.

The half-width of the gap L is 1 mm. The wall temperature in the inlet section T_e is taken equal to 423 K, which ensures a minimum rate of the chemical reaction in the considered time intervals and allows one to use a zero-degree-of-cure condition in the inlet section vicinity. The wall temperature T_w and the average flow velocity in the inlet section U_0 vary during parametric studies. The values of these characteristics and the corresponding dimensionless criteria are presented in Table 1. Distributions of the dimensionless velocity and temperature in the inlet section under the selected conditions are shown in Fig. 3. The velocity profiles are almost the same. The difference in the temperature profiles is related to dissipative effects.

Table 1. Values of dimensionless parameters of the problem

Condition	Re	W	Pe	Br	Da
U_0 = 0.05 m/s, T_w = 503 K	0.0010	0.0041	132.9	0. 0006	1.57
U_0 = 0.1 m/s, T_w = 503 K	0.0031	0.0031	265.8	0.0015	3.14
U_0 = 0.2 m/s, T_w = 503 K	0.0093	0.0023	531.6	0.0041	6.27
U_0 = 0.1 m/s, T_w = 473 K	0.0031	0.0031	265.8	0.0015	3.14
U_0 = 0.1 m/s, T_w = 423 K	0.0031	0.0031	265.8	0.0015	3.14

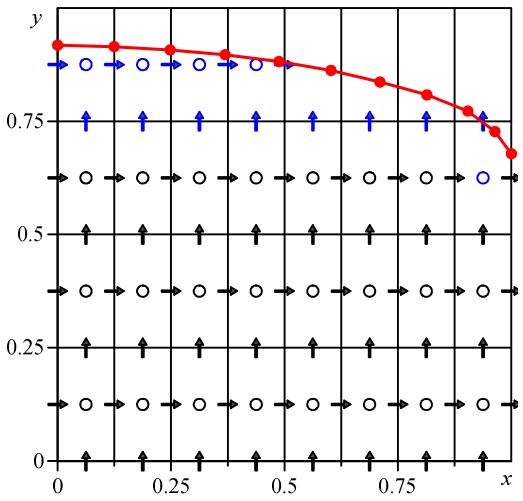

Fig. 2. A fragment of the computational grid with h_x = 1/8, h_y = 1/4 (○ – p pressure nodes, ↑ – v velocity nodes, → – u velocity nodes)

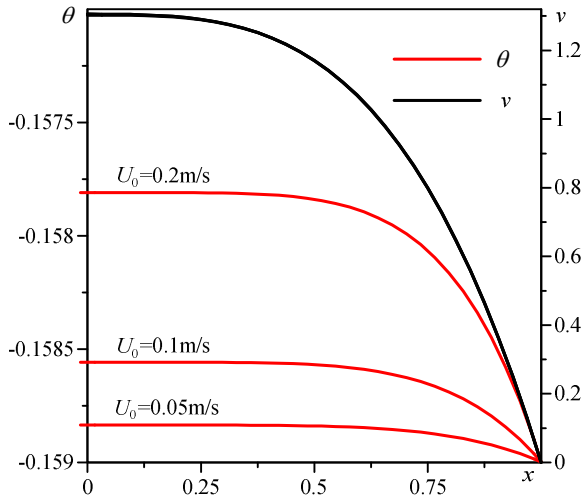

Fig. 3. Distribution of characteristics in the inlet section

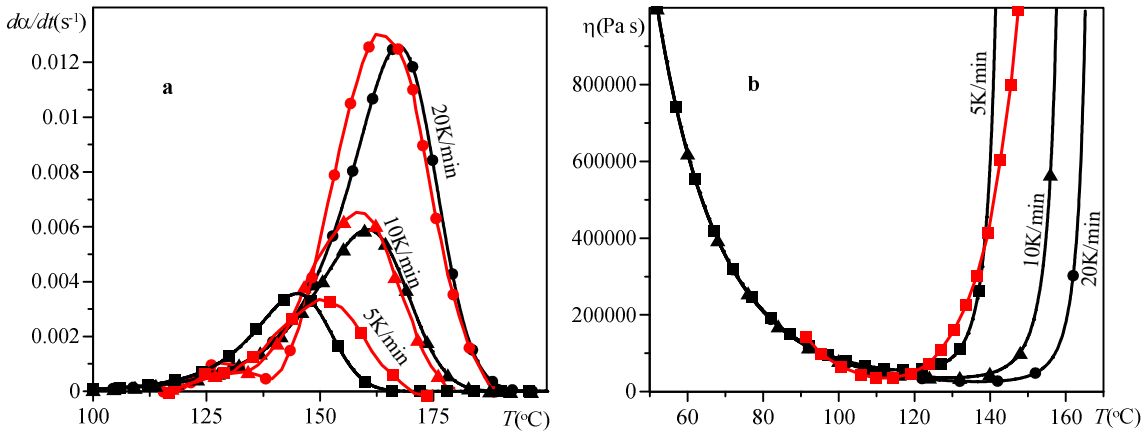

Fig. 4. Variation in the rate of cure (a) and viscosity (b) of the sample as a function of temperature (black lines indicate the calculated data; red lines, the experimental data [16])

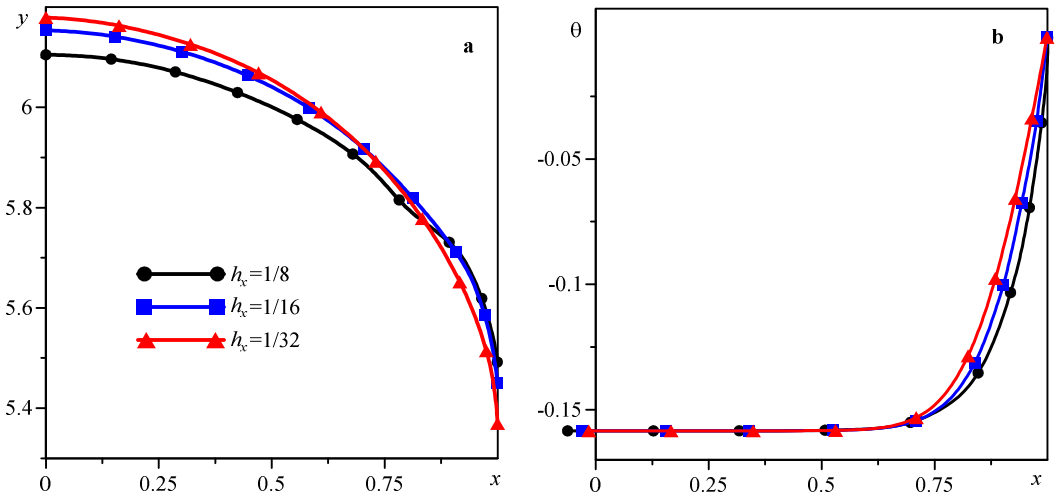

Fig. 5. Free surface shapes (a) and temperature distributions in section y = 3 (b) at time τ = 5 (U_0 = 0.1 m/s, T_w = 503 K)

In the first stage of the study, a model of the material curing in a small volume is tested assuming the uniform distribution of characteristics and, thus, providing the conditions of calorimetric experiments [16]. The material is heated from a temperature of -60°C at a given constant heating rate. Figure 4a illustrates a plot of the rate of cure versus temperature. Under the given conditions, there is almost no reaction at temperatures below 120°C. The apparent viscosity as a function of temperature is shown in Fig. 4b. The material has the lowest viscosity in the range of approximately 100–140°C. The numerical and experimental

data presented are in satisfactory agreement. Idealized nature of the mathematical model used and the computational algorithm peculiarities related to the elimination of the rheological model singularity at the gelation point provide an error when accounting for the conditions of the physical experiment and could be a reason for the differences between experimental and computed data.

The next stage of the study is devoted to verification of the approximation convergence of the computational algorithm developed for calculating plane channel filling with a non-Newtonian fluid with a free surface, taking into account the curing reaction. Figure 5 shows the free boundary shapes and a temperature distribution in section y = 3 at time $\tau = 5$ which are obtained on a sequence of grids with a spatial step of h_x = 1/8, 1/16, and 1/32 ($h_y = 2h_x$). The presented data confirm the convergence of the algorithm. The results reported in the next section are obtained with the regularization parameter $\varepsilon = 0.025$ and grid steps h_x = 1/32 and h_y = 1/16. The time step is determined by formula $\Delta\tau = 0.1h_x^2$. Calculations with fractional steps $\Delta\tau/2$ and $\Delta\tau/4$ at fixed h_x show that the difference in the coordinate of the free surface at x = 0 does not exceed 10^{-4} for the considered filling times.

4. Results and Discussion

Using the proposed algorithm, series of calculations are performed for the parameters presented in Table 1. All the flow characteristics in Figs. 3, 5 – 14 are presented in dimensionless form. The evolution of the free surface is shown in Fig. 6. The initially flat surface takes a convex shape over time and moves along the channel. The hotter the wall, the flatter the surface. As the surface changes its position, the material gradually warms up due to the heat transferred through the wall. As a result, a curing reaction proceeds in the heated layers.

Flow kinematics under curing conditions is shown in Fig. 7 at T_w = 503 K, T_e = 423 K, and U_0 = 0.1 m/s. The material is considered as cured if the extent of the reaction is greater than that at the gelation point. Streamlines flow around the region with the cured material and around the adjacent thin layer with increased viscosity. In this layer, the gelation point has not yet been attained, but the viscosity is much higher than that in the vicinity of the flow symmetry plane.

Distributions of flow characteristics at time τ = 15 are shown in Fig. 8. Near the lower boundary of the cured layer, the transverse flow is characterized by the highest intensity, and in the rest of the flow, its intensity is insignificant. Negative dimensionless temperature is due to the method of nondimensionalization. In the regions with negative θ, the dimensional temperature is less than T_w. The heaviest longitudinal velocity gradients are observed at some distance from the cured layer. This behavior is depicted in Fig. 9 that shows a longitudinal velocity distribution in section y = 5 (red line). In this section, three regions can be distinguished: a central “core” with small velocity gradients, a fixed cured layer on the wall, and a transition zone in between. The blue line indicates a distribution of the degree of cure in this section. In the central “core”, there is no significant increase in the degree of cure, while in the fixed layer, its value varies in the range of 0.4–1.0. Thus, even when the gelation point has not yet been attained (α_g = 0.7), the viscosity increases a lot, and the material behaves like a solid body under the given strain conditions. The yellow line indicates a viscosity distribution; the high viscosity in the central “core” is explained by low strain rates, and in the vicinity of the wall, it is a result of a high degree of cure. The low viscosity region is located in the transition zone. Analysis of the pressure distribution shows that the pressure is almost invariable in most of the flow except for the region near the lower part of the cured layer and the free surface vicinity.

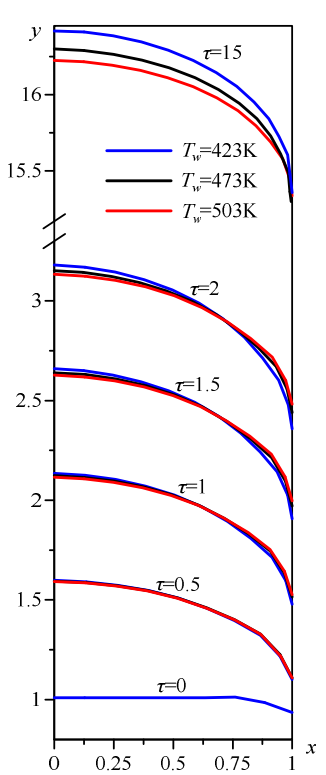

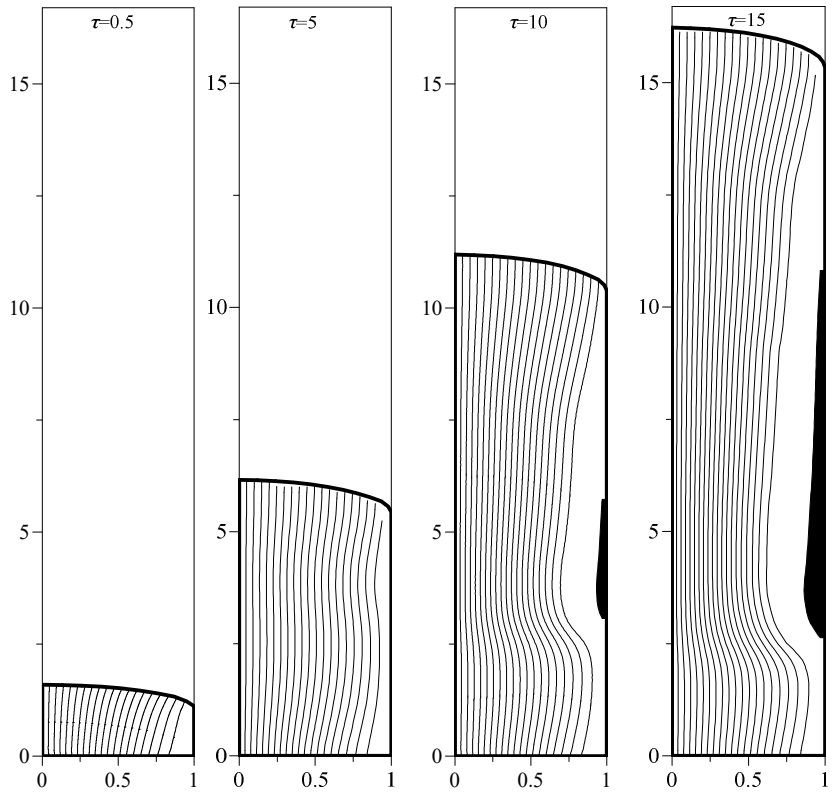

Fig. 6. Evolution of the free surface (U_0 = 0.1m/s) **Fig. 7.** Distributions of streamlines and cured layer at different time instants (U_0 = 0.1m/s, T_w = 503 K)

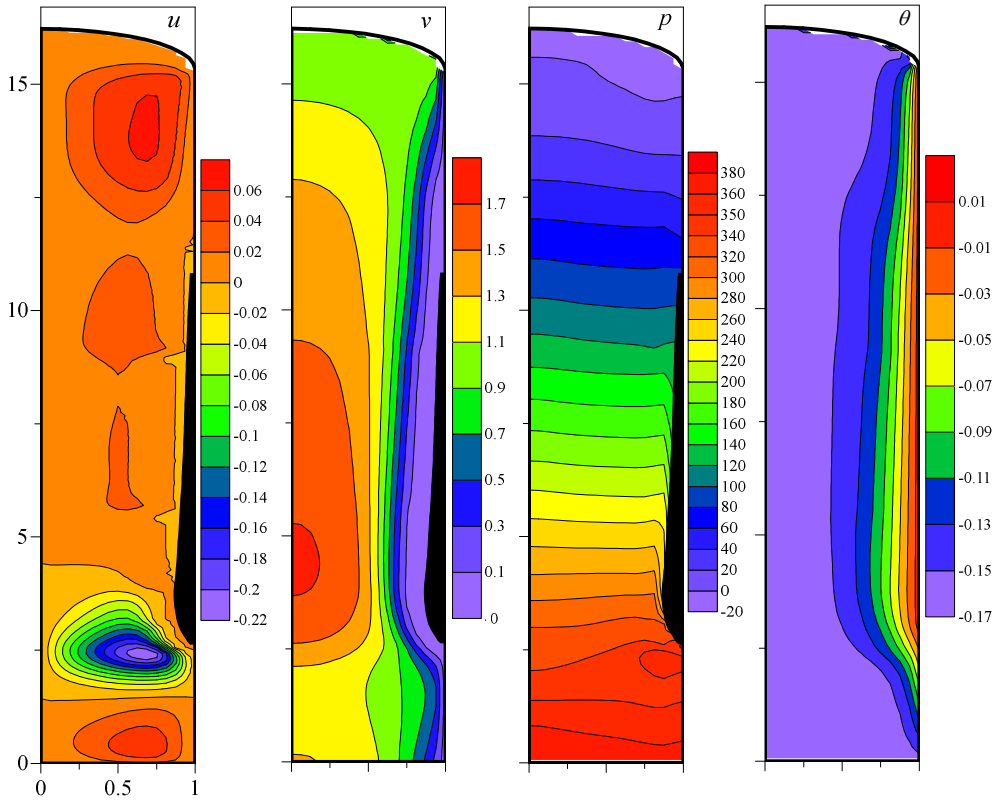

Fig. 8. Distributions of flow characteristics at $\tau = 15$ ($U_0 = 0.1$ m/s, $T_w = 503$ K)

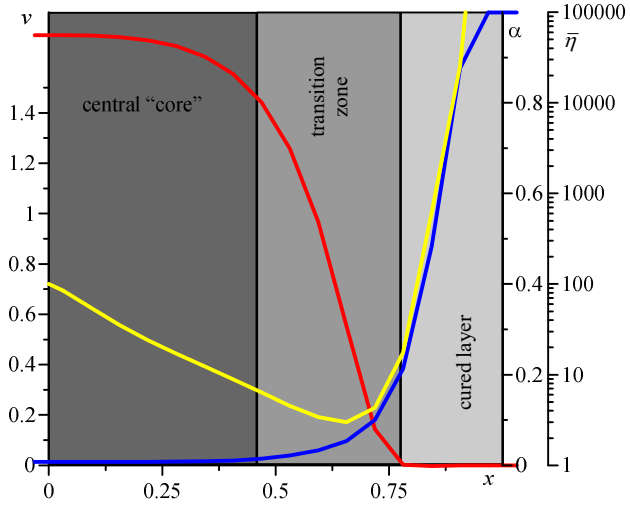

Fig. 9. Distribution of flow characteristics in section $y = 4$ at $\tau = 15$ ($U_0 = 0.1$ m/s, $T_w = 503$ K)

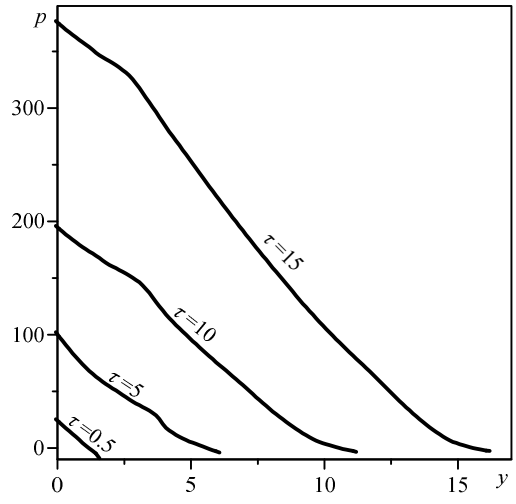

Fig. 10. Pressure distribution along the symmetry line at different time instants ($U_0 = 0.1$ m/s, $T_w = 503$ K)

Pressure distributions along the symmetry line at different times are shown in Fig. 10. At the initial stage of the filling (t = 0.5), the pressure decreases linearly. The linearity is broken over time as the cured layer forms.

Thus, the flow structure is characterized by low-viscosity layer formation along the solid wall due to the medium heating – the so-called "lubricating" layer, and a central "core" – the so-called "plug" zone. The "lubricating" layer shifts to the symmetry line in the course of time due to the growth of the fixed layer on the wall caused by curing. The "lubricating" layer is conditionally distinguished in terms of apparent viscosity values less than ten dimensionless units (Fig. 11). The selected area is characterized by high intensity of the strain rate at the given flow conditions and, as a consequence, by low viscosity.

When the wall temperature is not high enough to induce curing, a two-dimensional flow occurs in the free surface vicinity, and a one-dimensional steady flow, in the rest of the channel (Fig. 12). As the wall temperature increases, the effects of curing become apparent, and the "lubricating" layer starts to appear, which was discussed in detail earlier.

Pressure variation with time in the inlet section, which maintains a constant flow rate, is shown in Fig. 14a. At the initial stage of the filling ($\tau < \tau_1$), a higher wall temperature corresponds to a lower pressure in the inlet section due to the "lubricating" layer formation. However, in a case of $T_w = 507$ K at $\tau > \tau_1$, the cured layer formation on the wall leads to greater hydraulic resistance than that at $T_w = 200$°C, although the "lubricating" layer occurs in both cases.

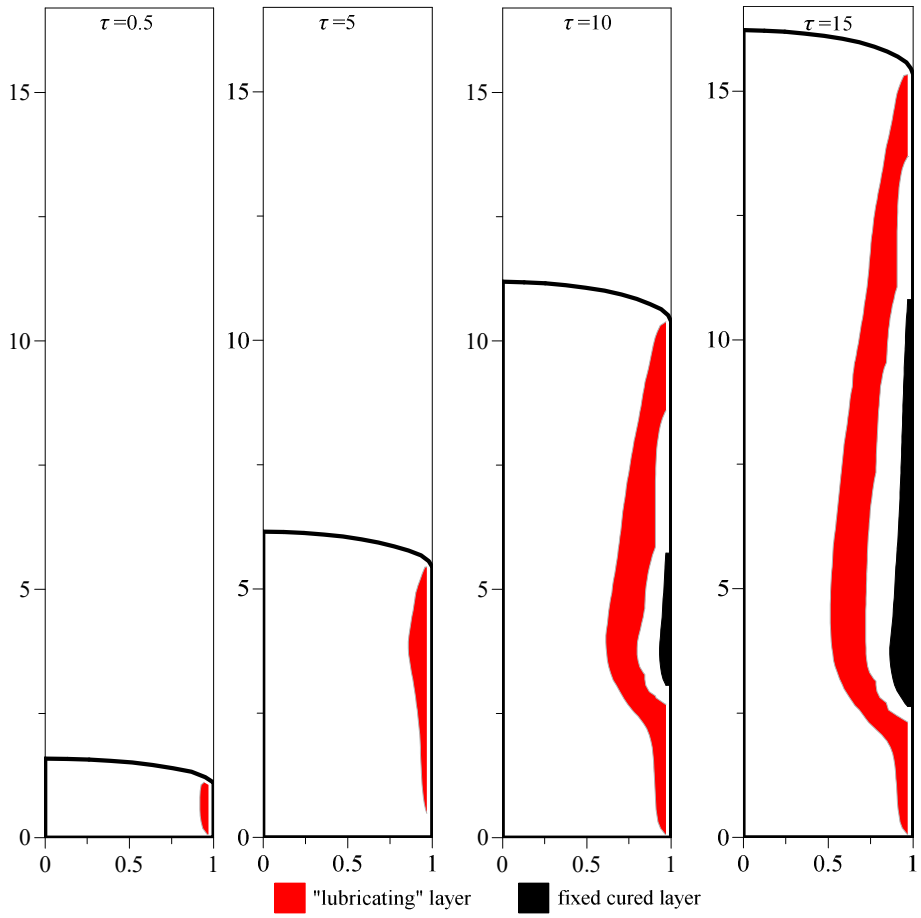

Fig. 11. Evolution of a "lubricating" layer (U_0 = 0.1 m/s, T_w = 503 K)

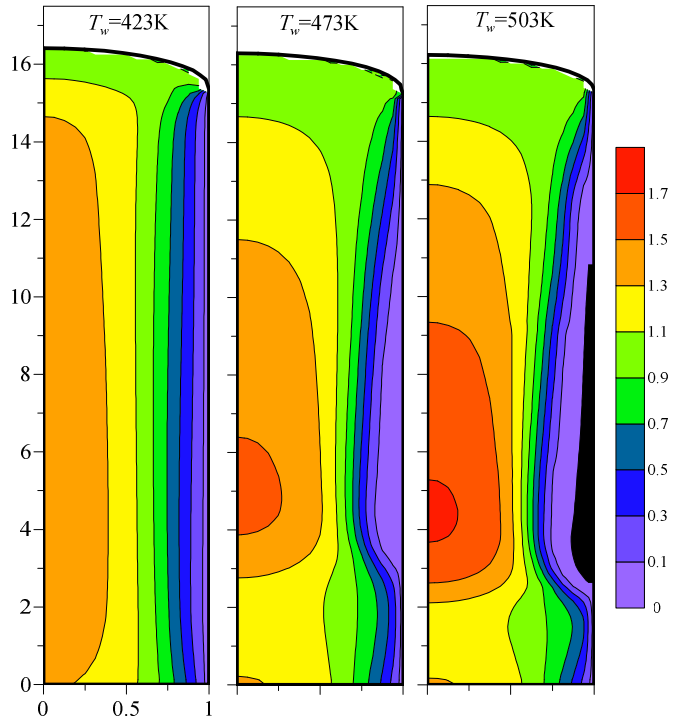

Fig. 12. Longitudinal velocity distribution at time τ = 15 (U_0 = 0.1 m/s)

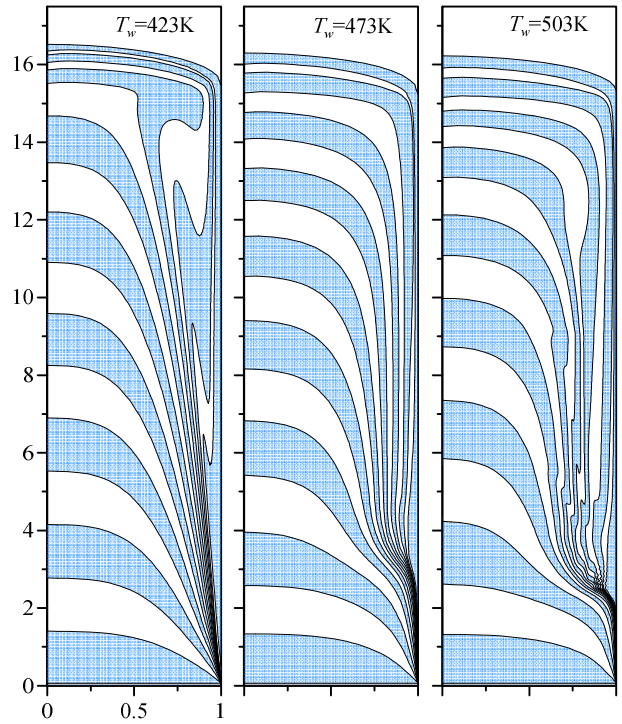

Fig. 13. Topograms of the mass distribution at time τ = 15 (U_0 = 0.1 m/s)

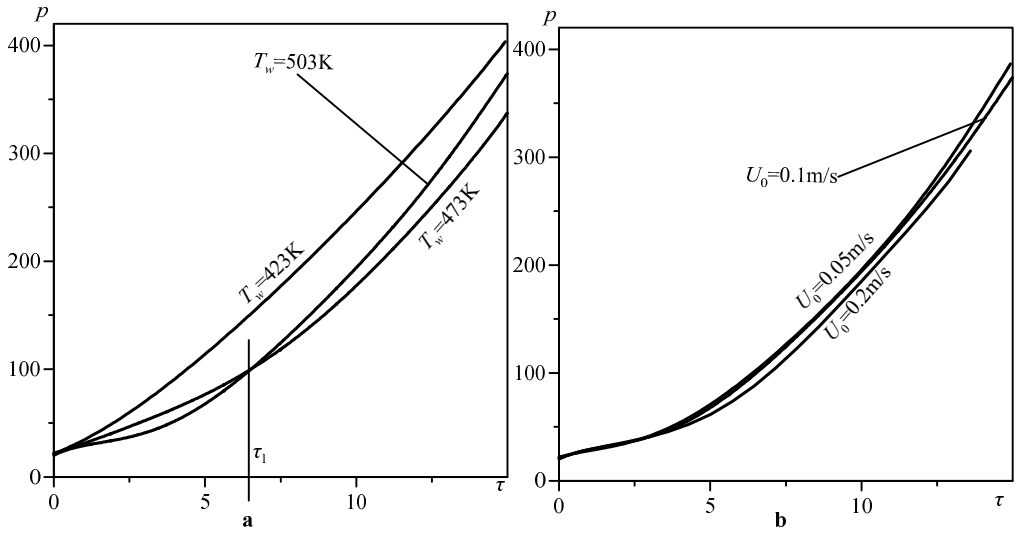

Fig. 14. Pressure in the inlet section as a function of time (a: $U_0 = 0.1$ m/s, b: $T_w = 503$ K)

Figure 13 shows the topograms of the mass distribution for liquid portions entering the channel sequentially within one dimensionless unit of time. In the figure, the portions are painted in different colors. For the case of low wall temperature, such a distribution corresponds to the fountain flow kinematics [3, 29]. As the temperature rises, the fountain effect weakens, and the distribution of the portions changes its behavior.

The parametric studies have shown that the average velocity in the inlet section varying in the range of 0.05 – 0.2 m/s does not lead to significant changes in the distribution of temperature and cured layer within the considered time interval. The dimensionless pressure variation in the inlet section is shown in Fig. 14b for various average velocities of the flow. The curves coincide qualitatively and quantitatively. However, the dimensional values would not be the same due to a difference in the scales.

5. Conclusion

A mathematical formulation of the problem of a non-Newtonian fluid flow during the plane channel filling at a given flow rate in the inlet section was proposed with account for curing of the liquid medium. An original numerical algorithm was developed on the basis of the finite volume method, and the Lagrangian method was used for determining the free boundary location. Distributions of flow kinematic characteristics were analyzed with respect to the given wall temperature and average velocity in the inlet section. The wall temperature T_w varied in the range from 423 to 503 K, and the average velocity in the inlet section U_0, from 0.05 to 0.2 m/s. Such a temperature range ensures the implementation of the process being studied for the material under consideration. Three characteristic zones were revealed in the flow of the curable fluid during the filling process: a fixed layer on the solid wall with a high degree of curing; a central “core” with an almost uniform distribution of characteristics; a transition zone between the central “core” and the fixed layer, which serves as a "lubricating" layer. Filling of the channel up to a height of 16 dimensionless units made it possible to fully observe the described flow structure. Analysis of the similarity criteria for the considered flow conditions showed that the fluid flows in a creeping regime (Re < 0.01); the temperature distribution was mainly affected by convective heat transfer (Pe > 100); the influence of dissipative heating and exothermic effect of the curing reaction was insignificant. The flow structure was determined by heating of the fluid through the wall, since the heating affected the rheological characteristics of the medium and the rate of the cured layer formation.

Author Contributions

E.I. Borzenko developed a mathematical model of the process and performed computational experiments. The calculated results were discussed and analyzed by both authors. All the authors participated in writing and editing of the manuscript.

Acknowledgments

Not Applicable.

Conflict of Interest

The authors declared no potential conflicts of interest concerning the research, authorship, and publication of this article.

Funding

The research is implemented at the expenses of the Russian Science Foundation (project No. 18-19-00021- П).

Data Availability Statements

The datasets generated and/or analyzed during the current study are available from the corresponding author on reasonable request.

Nomenclature

A, B	Constants in the kinetic equation [1/s]
Br	Brinkman number
c	Heat capacity [J/(kg K)]
c_0	Heat capacity scale [J/(kg K)]
C	Constant in the rheological model [Pa s]
C_1, C_2	Constants in the rheological model
Da	Damköhler number
E_a, E_b	Constants in the kinetic equation [J/mol]
g	Gravitational acceleration [m/s^2]
ΔH	Thermal effect of the chemical reaction [J/kg]
k	Constant in the rheological model
L	Half-width of the gap [m]
m, n	Constants in the kinetic equation
P	Pressure [Pa]
p	Dimensionless pressure
Pe	Peclet number
Re	Reynolds number
t	Time [s]
τ	Dimensionless time
T	Temperature [K]
T_e, T_w	Wall temperature near and far from the inlet section, respectively [K]
T_0	Temperature scale [K]
T_b	Constant in the rheological model [K]
$\mathbf{U}$	Velocity vector [m/s]
$\mathbf{u}=(u,v)$	Dimensionless velocity vector
U_0	Average velocity in the inlet section [m/s]
W	Dimensionless number
(x,y)	Cartesian coordinate system
α	Degree of cure
α_g	Degree of cure at the gelation point (above this point, the material loses its flow properties)
$\dot{\gamma}$	Intensity of the rate of strain [1/s]
ε	Regularization parameter
η	Apparent viscosity [Pa s]
$\overline{\eta}$	Dimensionless apparent viscosity
θ	Dimensionless temperature
λ	Thermal conductivity [W/(m K)]
ρ	Fluid density [kg/m^3]
σ	Constant in the rheological model [Pa]
Φ	Dissipation function [W/m^3]

References

[1] Mitsoulis, E., Fountain flow revisited: The effect of various fluid mechanics parameters, *AIChE J.*, 56(2), 2010, 1147-1162.
[2] Mavridis, H., Hrymak, A.N., Vlachopoulos, J., Mathematical modeling of injection mold filling: A review, *Adv. Polym. Technol.*, 6(4), 1986, 457-466.
[3] Coyle, D.J., Blake, J.W., Macosko, C.W., The kinematics of fountain flow in mold-filling, *AIChE J.*, 33(7), 1987, 1168-1177.
[4] Borzenko, E.I., Ryltsev, I.A., Shrager, G.R., Kinematics of Bulkley-Herschel fluid flow with a free surface during the filling of a channel, *Fluid Dyn.*, 52(5), 2017, 646-656.
[5] Borzenko, E.I., Ryltseva, K.E., Shrager, G.R., Free-surface flow of a viscoplastic fluid during the filling of a planar channel, *J. Nonnewton. Fluid Mech.*, 2018, 254, 12-22.
[6] Borzenko, E.I., Shrager, G.R., Effect of viscous dissipation on temperature, viscosity, and flow parameters while filling a channel, *Thermophys. Aeromechanics*, 21(2), 2014, 211-221.
[7] Tomashevsky, V.T., Yakovlev, V.S., Coupled problems of mechanics and chemical physics in the technology for producing composite polymer materials, *Mater. Phys. Mech.*, 8(1), 2009, 32-64.
[8] Malkin, A.Y., Kulichikhin, S.G., *Rheokinetics of curing*, Polymer Compositions Stabilizers/Curing, Springer-Verlag, 1991.
[9] Gillham, J.K., Formation and properties of thermosetting and high T_g polymeric materials, *Polym. Eng. Sci.*, 26(20), 1986, 1429-1433.
[10] Urbaniak, M., Grudzinski, K., Time-temperature-transformation (TTT) cure diagram for EPY epoxy system, *Polimery*, 52(2), 2007, 117-126.
[11] Muc, A., Romanowicz, P., Chwał, M., Description of the Resin Curing Process - Formulation and Optimization, *Polymers (Basel)*, 11(127), 2019, 1-22.
[12] Domínguez, J.C., *Rheology and curing process of thermosets*, Chapter 4, Thermosets. Elsevier, 2018.
[13] Bont, M., Barry, C., Johnston, S., A review of liquid silicone rubber injection molding: Process variables and process modeling, *Polym. Eng. Sci.*, 61(2), 2021, 331-347.
[14] Wittemann, F., Maertens, R., Kärger, L., Henning, F., Injection molding simulation of short fiber reinforced thermosets with anisotropic and non-Newtonian flow behavior, *Compos. Part A Appl. Sci. Manuf.*, 124(105476), 2019, 1-9.
[15] Wittemann, F., Maertens, R., Bernath, A., Hohberg, M., Kärger, L., Henning, F., Simulation of Reinforced Reactive Injection Molding with the Finite Volume Method, *J. Compos. Sci.*, 2(5), 2018, 1-16.
[16] Tran, N.T., Gehde, M., Creating material data for thermoset injection molding simulation process, *Polym. Test.*, 73, 2019, 284-292.
[17] Hong, Y.G., Lee, S., 3-D Modeling of Epoxy Reaction Molding Process for GIS Spacer, *Polym. Korea*, 45(6), 2021, 940-947.
[18] Teng, S-Y, Hwang, S-J., Simulations and experiments of three-dimensional paddle shift for IC packaging, *Microelectron. Eng.*, 85(1), 2008, 115-125.
[19] Khor, C.Y., Abdullah, M.Z., Lau, C-S, Azid, I.A., Recent fluid–structure interaction modeling challenges in IC encapsulation – A review, *Microelectron. Reliab.*, 54(8), 2014, 1511-1526.
[20] Lipanov, A.M., Alies, M.Yu., Konstantinov, Yu.N., Numerical simulation of creep flow for non-Newtonian fluids with free interface, *Mat. Modelirovanie*, 5(7), 1993, 3–9.
[21] Kamal, M.R., Sourour, S., Kinetics and thermal characterization of thermoset cure, *Polym. Eng. Sci.*, 13(1), 1973, 59-64.
[22] Cross, M.M., Rheology of non-Newtonian fluids: A new flow equation for pseudoplastic systems, *J. Colloid Sci.*, 20(5), 1965, 417-437.
[23] Williams, M.L., Landel, R.F., Ferry, J.D., The Temperature Dependence of Relaxation Mechanisms in Amorphous Polymers and Other Glass-forming Liquids, *J. Am. Chem. Soc.*, 77(14), 1955, 3701-3707.
[24] Castro, J.M., Macosko, C.W., Studies of mold filling and curing in the reaction injection molding process, *AIChE J.*, 28(2), 1982, 250-260.
[25] Patankar, S V., *Numerical Heat Transfer and Fluid Flow*, Hemisphere Pub. Corp, 1980.
[26] Vasenin, I.M., Sidonskii, O.B., Shrager, G.R., Numerical solution of the problem on the movement of a viscous fluid with a free surface, *Dokl. Akad. Nauk. SSSR*, 217(2), 1974, 295-298.
[27] Yakutenok, V.A., Borzenko, E.I., Numerical simulation of viscous incompressible liquid with free interface using the SIMPLE method, *Mat. Modelirovanie*, 19(3), 2007, 52-58.
[28] Frigaard, I.A., Nouar, C., On the usage of viscosity regularisation methods for visco-plastic fluid flow computation, *J. Nonnewton. Fluid Mech.*, 127(1), 2005, 1-26.
[29] Borzenko, E.I., Shrager, G.R., Flow of a Non-Newtonian Liquid with a Free Surface, *J. Eng. Phys. Thermophys.*, 89(4), 2016, 902-910.

ORCID iD

E.I. Borzenko https://orcid.org/0000-0001-6264-1776
G.R. Shrager https://orcid.org/0000-0002-2485-8517

How to cite this article: Borzenko E.I., Shrager G.R. Flow structure when filling a channel with a curable liquid, *J. Appl. Comput. Mech.*, 9(1), 2023, 195–204. https://doi.org/10.22055/jacm.2022.40757.3648